

the first minimum occurs just after the change of curvature while the second occurs further downstream on the parallel section. The minima appear to be of comparable values in the particular cases shown.

Nose profiles having a more bluff aspect ( $a/t=2$ ,  $l/t=2$ ) show a very much stronger minimum  $\lambda$  at the further aft position on the surface, the particular cases considered indicating that separation would occur on the elliptical nose ( $a/t=2$ ) and the smaller nose arc ( $r/t=0.25$ ,  $l/t=2$ ) profiles. Where the nose profile has a more slender aspect ( $a/t=8$ ,  $l/t=8$ ) the minimum at the more forward position is stronger.

The variation of the minimum value of  $\lambda$  with the nose slenderness parameters  $a/t$  and  $l/t$  is shown in Fig. 3, separate curves denoting the minima at more forward or more aft positions. For the circular arc profiles it is seen that the tendency to separate may be minimized by selecting an intermediate value of  $l/t$  ( $l/t=4.0$  giving  $-\lambda_{\max}=3.6$  for  $r/t=0.5$  and  $l/t=4.6$  giving  $-\lambda_{\max}=3.2$  for  $r/t=0.25$ ) such that the minimum  $\lambda$  at both positions is the same. It seems that the result is not strongly sensitive to the value of  $r/t$  in the range  $0.25 < r/t < 0.5$  considered. If a greater margin to avoid separation is required, then an elliptical nose with  $a/t > 5.0$  should be used when  $(-\lambda_{\max}) < 3.0$  can be obtained. Experiments with a flat plate with a thickness Reynolds number between  $1.5 \times 10^4$  and  $5.0 \times 10^4$  and having an elliptical leading edge with  $a/t=4.0$  were found to give no problems in the leading-edge area even when the plate was subjected to intense acoustical disturbances.<sup>2</sup>

### III. Conclusions

The tendency for flow separation in the leading-edge region of a flat surface can be minimized using double arc contours with  $r/t=0.25$  and  $l/t=4.6$ . Where a greater margin for boundary-layer separation near the nose is required, an elliptical leading edge with  $a/t > 5.0$  should be used.

### Acknowledgment

The support of the National Sciences Foundation and the Office of Naval Research while the author was at the Massachusetts Institute of Technology is gratefully acknowledged.

### References

- Chang, P. K., *Separation of Flow*, Pergamon Press, London, 1970.
- Shapiro, P. J., "The Influence of Sound Upon Laminar Boundary Layer Instability," Acoustics and Vibration Laboratory, Massachusetts Institute of Technology, Rept. No. 83458-83560-1, Sept. 1977.
- De Metz, F. C. and Casarella, M. J., "An Experimental Study of the Intermittent Properties of the Boundary Layer Pressure Field During Transition on a Flat Plate," Dept. of the Navy, NSRDC Rept. 4140, Nov. 1973.
- Kobashi, Y., Hayakawa, M., and Nakagawa, K., "Development of Disturbances in Unsteady Boundary Layers," *Symposium on Unsteady Aerodynamics*, Vol. 1, edited by R. B. Kinney, Arizona Board of Regents, Tuscon, Ariz., 1975, pp. 131-153.
- Schubauer, G. B. and Klebanoff, P. S., "Contributing on the Mechanics of Boundary Layer Transition," National Advisory Committee for Aeronautics, Technical Rept. No. 1289, 1956.
- Knapp, C. F. and Roache, P. J., "A Combined Visual and Hot-Wire Anemometer Investigation of Boundary Layer Transition," *AIAA Journal*, Vol. 6, 1968, pp. 29-37.
- Milgram, J. H., "Slender Foil Computer Program AIR," Massachusetts Institute of Technology, Dept. of Ocean Engineering, private communication, 1975.
- Schlichting, H., *Boundary Layer Theory*, 6th ed., McGraw Hill, New York, 1968.
- Walz, A., "Ein neuer Ansatz für das Geschwindigkeitsprofil der laminaren Reihengsschicht," *Lilienthal-Bericht*, Vol. 141, 1941.

## Effects of Swirl on the Subcritical Performance of Convergent Nozzles

20010  
20016

P. W. Carpenter\*  
University of Exeter, Exeter, England

### Introduction

SCHWARTZ<sup>1,2</sup> has advocated the use of swirl as a possible method of noise reduction for turbojet and turbofan engines. His experimental data show considerable noise attenuation. On the other hand, the experimental results obtained by Lu et al.<sup>3</sup> and Whitfield<sup>4</sup> appear to be less promising. An important factor in assessing the suitability of swirl as a noise suppression device is the magnitude of the thrust loss incurred. Accordingly, a relatively simple method of estimating the effects of swirl on the mass flux and thrust of a subcritical convergent nozzle flow is presented below.

Some previous theoretical work has been reported on subcritical swirling flows in nozzles. For instance, Bussi<sup>5</sup> compared Mach number distributions in a convergent-divergent nozzle obtained by numerical methods with the predictions of quasicylindrical theory. An approximate method is presented by Lu et al.,<sup>3</sup> who apparently assume that the swirl angle remains constant across a nozzle section. It is shown herein that this method leads to substantially larger estimates of the thrust loss as compared to the present method. Experimental measurements of thrust and mass flux for subcritical swirling nozzle flows have been reported by Whitfield.<sup>4</sup> These experiments were carried out at Rolls-Royce, Bristol, using single- and double-stage fixed-vane swirlers. Some of the data obtained are compared to theoretical predictions.

### Analysis

It is assumed that the flow at the nozzle exit section is equivalent to a swirling flow in an infinitely long cylindrical duct. This is the so-called quasicylindrical assumption, which is analogous to the familiar one-dimensional theory for nonswirling nozzle flows. Furthermore, it is assumed that the swirl is produced by fixed vanes. This implies that for an inviscid non-heat-conducting gas the entropy and stagnation enthalpy are uniformly constant throughout the flow. Under these conditions Carpenter and Johannesen<sup>6</sup> have shown that the Crocco vorticity theorem reduces to

$$\frac{v}{r} \frac{d(rv)}{dr} + w \frac{dw}{dr} = 0 \quad (1)$$

where  $v$  and  $w$  are, respectively, the tangential and axial velocity components at the nozzle exit and  $r$  the radial coordinate. Integration of Eq. (1) gives

$$w = \left( q_{\text{ex}}^2 - v_{\text{ex}}^2 + 2 \int_r^{R_{\text{ex}}} \frac{v}{r'} \frac{d(r'v)}{dr'} dr' \right)^{1/2} \quad (2)$$

where  $q^2 = v^2 + w^2$ , subscript ex indicates conditions at the nozzle lip and  $R_{\text{ex}}$  is the radius of the nozzle exit section.

The pressure,  $p$  and density  $\rho$  at the nozzle exit are obtained from the isentropic flow relations, namely

$$\left( \frac{p}{p_0} \right)^{\gamma-1} = \left( \frac{p}{p_0} \right)^{(\gamma-1)/\gamma} = 1 - \frac{\gamma-1}{\gamma+1} (W^2 + V^2) \quad (3)$$

Received May 8, 1979; revision received Nov. 7, 1979. Copyright © American Institute of Aeronautics and Astronautics, Inc., 1979. All rights reserved.

Index categories: Nozzle and Channel Flow; Subsonic Flow.

\*Lecturer, Dept. of Engineering Science. Member AIAA.

where  $W = w/a_*$ ,  $V = v/a_*$ ,  $a_*$  is the critical speed of sound,  $\gamma$  is the ratio of the specific heats, and subscript 0 denotes stagnation conditions.

The quantities of most practical significance in assessing nozzle performance are the mass flux, impulse function, and thrust. Nondimensional coefficients for these three quantities can be defined as follows:

$$\begin{aligned} C_m &= 2 \int_0^{R_{ex}} \rho w r dr / \rho_* a_* R_{ex}^2, \\ C_{nx} &= 2 \int_0^{R_{ex}} (p + \rho w^2) r dr / (p_* + \rho_* a_*^2) R_{ex}^2, \\ C_t &= t / \rho_* a_*^2 \pi R_{ex}^2 \end{aligned} \quad (4)$$

where  $\rho_*$  and  $p_*$  are the density and pressure corresponding to  $a_*$  and  $t$  is the thrust.

The thrust generated by a nozzle attached to a turbojet engine which is moving with forward speed  $V_F$  is given to good approximation by

$$t = 2\pi \int_0^{R_{ex}} (p + \rho w^2) r dr - 2\pi V_F \int_0^{R_{ex}} \rho w r dr - \pi p_A R_{ex}^2 \quad (5)$$

where  $p_A$  is the ambient pressure. Using Eq. (5) together with definitions Eq. (4) we find that

$$C_t = \frac{\gamma+1}{\gamma} C_{nx} - \frac{V_F}{a_*} C_m - \frac{1}{\gamma} \left( \frac{\gamma+1}{2} \right)^{\gamma/(\gamma-1)} \frac{p_A}{p_0} \quad (6)$$

If the back-pressure ratio,  $p_A/p_0$ , is given, then the non-dimensional total velocity at the nozzle lip, i.e.,  $q_{ex}/a_*$ , can be determined from Eq. (3). Hence, if the swirl profile at nozzle exit is given, the axial velocity can be determined from Eq. (2). The density and pressure distributions can then be determined from Eq. (3). With the axial velocity, density, and pressure distributions determined, the coefficients  $C_m$  and  $C_{nx}$  can be evaluated by numerical quadrature.

In the case of weak swirl analytical expressions can be obtained for  $C_m$  and  $C_{nx}$  by following a procedure similar to that described in Refs. 6 and 7. Accordingly, the right-hand side of Eq. (2) is expanded and terms of  $O(V_{ex}^4)$  neglected. Approximate expressions for  $\rho/\rho_0$  and  $p/p_0$  are obtained from Eq. (3) by expanding and neglecting terms of  $O(V_{ex}^4)$ . These approximate expressions for  $W$ ,  $\rho/\rho_0$ , and  $p/p_0$  are substituted into the integrands in definitions (4) and the integrations carried out, again neglecting terms of  $O(V_{ex}^4)$ , to obtain the following approximate expressions:

$$C_m = Q_{ex} \left( \frac{\gamma+1}{2} \Lambda \right)^{1/(\gamma-1)} \left( 1 - \frac{2}{(\gamma+1)\Lambda} \epsilon_m \right) \quad (7)$$

$$\begin{aligned} C_{nx} &= \frac{1}{2} (1 + Q_{ex}^2) \left( \frac{\gamma+1}{2} \Lambda \right)^{1/(\gamma-1)} \\ &\times \left( 1 - \frac{2}{\gamma+1} \left( \frac{1}{\Lambda} + \frac{\gamma-1}{1+Q_{ex}^2} \right) \epsilon_m \right) \end{aligned} \quad (8)$$

where

$$Q = q/a_*, \quad \Lambda = 1 - \frac{\gamma-1}{\gamma+1} Q_{ex}^2,$$

$$\epsilon_m = \int_0^1 V^2 \zeta d\zeta \quad \text{and} \quad \zeta = r/R_{ex}$$

An approximate analytical expression for the thrust can be obtained by using Eqs. (7) and (8) together with Eq. (6). For example, the coefficient of specific static thrust is given by

$$\frac{C_{ts}}{C_m} = \frac{1}{\gamma} \left( \frac{\gamma+1}{2} \right) \frac{1}{Q_{ex}} \left( 1 + Q_{ex}^2 - \Lambda - \frac{2\gamma}{\gamma+1} \epsilon_m \right) \quad (9)$$

## Results and Discussion

Accurate values of  $C_m$  and  $C_{ts}/C_m$  have been computed for two families of swirl distributions. The first of these is defined as follows:

$$V = \Omega \zeta; \quad 0 \leq \zeta \leq \zeta_c; \quad V = \Omega \zeta_c^2 / \zeta; \quad \zeta_c \leq \zeta \leq 1 \quad (10)$$

This represents an "inner-biased" swirling flow with a core, of radius  $\zeta_c R_{ex}$ , which is in solid-body rotation; outside the core there is free-vortex flow. The parameters  $\Omega$  and  $\zeta_c$  can both be varied. The second family of swirl distributions is defined as follows:

$$V = 0; \quad 0 \leq \zeta \leq \zeta_c^*; \quad V = \frac{\zeta - \zeta_c^*}{1 - \zeta_c^*} V_{ex}; \quad \zeta_c^* \leq \zeta \leq 1 \quad (11)$$

This represents an "outer-biased" swirling flow with a nonswirling core of radius  $\zeta_c^* R_{ex}$ , surrounded by an annulus of swirling flow. Again, two parameters,  $V_{ex}$  and  $\zeta_c^*$ , can be varied. This type of flow is similar to those investigated experimentally by Lu et al. and Whitfield, who used annuli of swirler blades to produce the swirl.

Values of  $C_m$  and  $C_{nx}$  were determined by numerical quadrature for various swirl levels and types of swirling flow. In Fig. 1 calculated points representing these values of  $C_m$  are plotted against the swirl parameter  $\epsilon_m$  for various back-pressure ratios. Similarly, calculated points representing values of  $C_{ts}/C_m$ , obtained by using Eq. (6) and the computed values of  $C_m$  and  $C_{nx}$ , are plotted in Fig. 2. It can be seen from both Figs. 1 and 2 that the calculated points corresponding to a particular value of  $p_A/p_0$  almost fall on a single curve, even at high swirl levels. This suggests that to a good approximation  $\epsilon_m$  may be regarded as a universal swirl parameter for subcritical swirling nozzle flows; a similar result was found in the supercritical case.<sup>7</sup> The solid curves drawn through the calculated points in Figs. 1 and 2 are intended to represent these notional "universal" curves. Also plotted as dashed lines in Figs. 1 and 2 are the variations of  $C_m$  and  $C_{ts}/C_m$  with  $\epsilon_m$  according to Eqs. (7) and (9), respectively. It can be seen that Eqs. (7) and (9) appear to be reasonable approximations at moderate swirl intensities.

Lu et al.<sup>3</sup> carried out noise measurements on swirling jets but did not measure thrust. Instead, they estimated the thrust

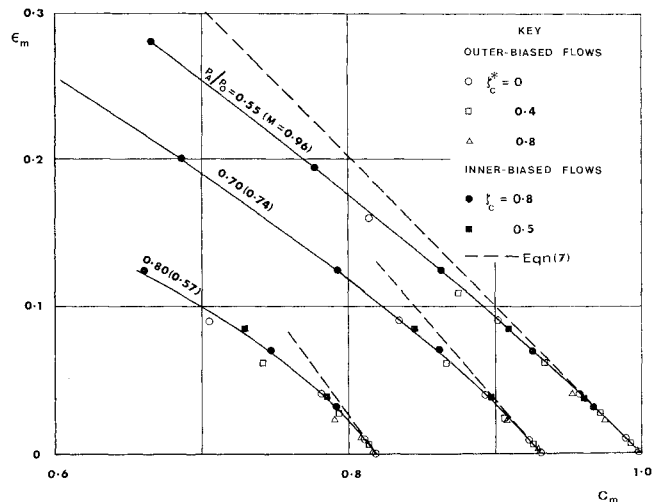


Fig. 1 Variation of mass-flux coefficient with swirl intensity,  $\gamma = 1.4$ .

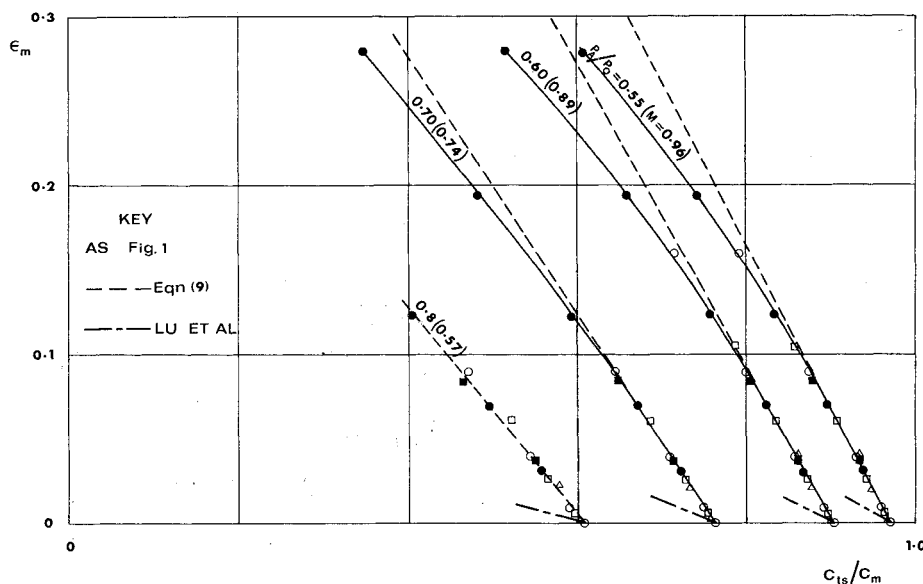


Fig. 2 Variation of static specific-thrust coefficient with swirl intensity,  $\gamma = 1.4$ .

Table 1 A comparison of calculated values and experimental data

$p_A/p_0$	$\alpha_{ex}$ , deg	$C_m/C_{m0}$		$(C_t/C_m)/(C_t/C_m)_0$	
		Theory	Experiment	Theory	Experiment
0.571	23	0.98	0.99	0.98	0.98
0.556	40	0.93	0.92	0.95	0.97

produced by the swirling jet by using the approximate theory previously mentioned. In Fig. 2 curves are plotted which represent the predictions of Lu et al. for the case of outer-biased swirling flow with  $\zeta_c^* = 0.8$ . These curves are calculated from the appropriate curve in Fig. 17 of Ref. 3. It can be seen from Fig. 2 that the approximate method of Lu et al. leads to substantially larger reductions in specific thrust as compared to the present theory. As a specific example, consider a flow with  $p_A/p_0 = 0.55$  and a swirl angle  $\alpha_{ex} = \arctan(V_{ex}/W_{ex}) = 25$  deg. The present theory predicts a reduction of 1% in specific static thrust compared to the no-swirl case. The comparable figure according to Lu et al. is approximately 3.5%. This is a significant difference when considering swirl as a possible noise-suppression technique.

In Table 1 the present numerical results are also compared with some of Whitfield's experimental results for outer-biased swirling flows with  $\zeta_c^* = 0.6$ . In the case of the higher swirl angle some allowance has been made for the fact that the swirl-angle distribution is given at 0.5 diameters downstream of nozzle exit. It can be seen that there is reasonable agreement between the theoretical and experimental values.

In practice, it would be more natural to specify the swirl distribution immediately downstream of the swirler vanes rather than at the nozzle exit. However, upstream axial and swirl velocity profiles corresponding to particular exit conditions can be determined by following the method described in Ref. 6. Also, by following the method described in Ref. 7, the analysis can be easily extended to swirling flows with nonuniform stagnation enthalpy and/or entropy distributions, e.g., swirling flows produced by rotating blades.

## References

- <sup>1</sup>Schwartz, I. R., "Jet Noise Suppression by Swirling the Jet Flow," AIAA Paper 73-1003, 1973.
- <sup>2</sup>Schwartz, I. R., "Minimization of Jet and Core Noise of a Turbojet Engine by Swirling the Exhaust Flow," AIAA Paper 75-503, 1975.

<sup>3</sup>Lu, H. Y., Ramsay, J. W., and Miller, D. L., "Noise of Swirling Exhaust Jets," *AIAA Journal*, Vol. 15, May 1977, pp. 642-646.

<sup>4</sup>Whitfield, O. J., "Novel Schemes for Jet Noise Control," Ph.D. Thesis, Engineering Dept., Cambridge University, 1975.

<sup>5</sup>Bussi, G., "Analisi Numerica di Flussi Vorticosi in Ugelli," Istituto di Macchine e Motori per Aeromobili, Torino, Pub. No. 166, 1974.

<sup>6</sup>Carpenter, P. W. and Johannesen, N. H., "An Extension of One-Dimensional Theory to Inviscid Swirling Flow Through Choked Nozzles," *Aeronautical Quarterly*, Vol. 26, May 1975, pp. 71-87.

<sup>7</sup>Carpenter, P. W., "A General One-Dimensional Theory of Compressible Inviscid Swirling Flows in Nozzles," *Aeronautical Quarterly*, Vol. 27, Aug. 1976, pp. 201-216.

## J80-108 Free-Molecule Normal-Momentum Transfer at Satellite Surfaces

20013

Eldon L. Knuth\*

University of California, Los Angeles, Calif.

**F**ORCES due to free-molecule normal-momentum transfer at satellite surfaces are of great interest not only because those arising from collisions with atmospheric particles contribute to drag but also because those arising from asymmetric jet impingements introduce additional needs for attitude control. Hence a satellite designer would like to be able to predict these forces for a wide variety of particle species, surface materials, surface roughnesses, and surface contaminants, and for a wide range of particle energies, surface temperatures, and surface coverages.

Received July 10, 1979; revision received Oct. 22, 1979. Copyright © American Institute of Aeronautics and Astronautics, Inc., 1979. All rights reserved.

Index category: Rarefied Flows.

\*Professor of Engineering and Applied Science, Chemical, Nuclear and Thermal Engineering Dept. Consultant, Defense and Space Systems Group, TRW Inc., Redondo Beach, Calif. Associate Fellow AIAA.